

# Resonant three-body physics in two spatial dimensions

K. Helfrich and H.-W. Hammer

*Helmholtz-Institut für Strahlen- und Kernphysik (Theorie)*

*and Bethe Center for Theoretical Physics,*

*Universität Bonn, 53115 Bonn, Germany*

(Dated: May 19, 2011)

## Abstract

We discuss the three-body properties of identical bosons exhibiting large scattering length in two spatial dimensions. Within an effective field theory for resonant interactions, we calculate the leading non-universal corrections from the two-body effective range to bound-state and scattering observables. In particular, we compute the three-body binding energies, the boson-dimer scattering properties, and the three-body recombination rate for finite energies. We find significant effective range effects for three-body observables in the vicinity of the unitary limit. The implications of this result for future experiments are briefly discussed.

## I. INTRODUCTION

In the last few years, ultracold quantum gases have become a versatile tool to investigate few- and many-body phenomena in strongly interacting quantum systems. With the help of Feshbach resonances, the atomic interaction strength can be changed at will. This allows, for example, for the investigation of the BCS-BEC crossover in Fermi gases, the creation of molecules, the observation of the Efimov effect and of other universal phenomena (see, e.g., [1, 2] and references therein). The possibility of using optical lattices makes them also interesting for the simulation of condensed matter problems such as the Hubbard model [3]. Special trap geometries allow for the creation of lower-dimensional systems. They can, for example, help to understand high-temperature superconductivity which is a two-dimensional ( $2d$ ) problem. Moreover,  $2d$  systems are interesting on their own since their behavior can be qualitatively different from three dimensions.

Here, we concentrate on few-body phenomena in ultracold atomic gases with large scattering length. Such phenomena are of great interest because they are insensitive to the details of the interaction at short distances. They can be described in an expansion around the unitary limit. This limit refers to an idealized system where the range of the interaction is taken to zero and the scattering length  $a$  is infinite. To leading order in this expansion, the low-energy observables are universal. They are determined by the scattering length  $a$  of the particles alone. The leading non-universal corrections are due to the effective range of the interaction. In the current paper, we focus on these corrections. Since there is no Efimov effect [4] in two dimensions [5, 6], three-body interactions are suppressed and enter only at higher orders.

The definition of the scattering length  $a$  in  $2d$  is ambiguous since  $\cot \delta$  diverges logarithmically as the wave number  $k$  approaches zero and different conventions are used in the literature. We follow the conventions of Verhaar et al. [7], in which the effective range expansion of the scattering phase shift is given by

$$\cot \delta(k) = \frac{2}{\pi} \left\{ \gamma_E + \ln \left( \frac{ka}{2} \right) \right\} + \frac{r^2}{2\pi} k^2 + \mathcal{O}(k^4), \quad (1)$$

where  $\gamma_E \simeq 0.577216$  is Euler's constant. Note that the scattering length in two dimensions is always positive.

In the limit  $a \gg |r|$ , the binding energy of the shallow dimer is universal,

$$E_2 = 4e^{-2\gamma_E} \frac{\hbar^2}{ma^2} + \mathcal{O}(r^2/a^2). \quad (2)$$

The binding energies of three- and four-body states in this limit have been calculated by various groups and are also universal [5, 6, 8–11]. Since there is no other parameter in the problem, the energies must be multiples of the dimer energy. There are two three-body bound states which were first calculated by Bruch and Tjon [5]. Their binding energies are [8]

$$E_3^{(1)} = 1.2704091(1) E_2 \quad \text{and} \quad E_3^{(0)} = 16.522688(1) E_2, \quad (3)$$

where the number in parentheses indicates the numerical error in the last quoted digit. The first calculation of the four-body bound states in  $2d$  was carried out by Platter et al. [9]. They found also two universal bound states with binding energies

$$E_4^{(1)} = 25.5(1) E_2 \quad \text{and} \quad E_4^{(0)} = 197.3(1) E_2. \quad (4)$$

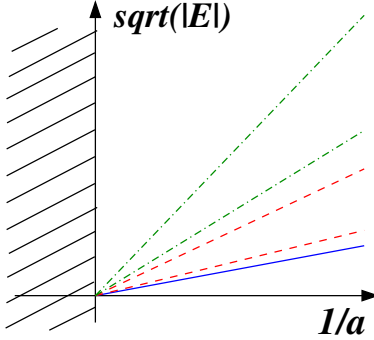


FIG. 1: (Color online) Spectrum of universal two-, three-, and four-body states in two spatial dimensions as a function of the inverse scattering length  $1/a$ .

These results were later confirmed in Ref. [10]. In Fig. 1, we illustrate the scattering length dependence of this spectrum. The universal few-body states do not cross the continuum threshold  $E = 0$  for any finite value of the scattering length. In contrast to three dimensions, the  $2d$  universal states can therefore not be observed as zero-energy resonances in few-body recombination.

For large values of  $N \gg 1$ , one can derive the universal properties of shallow  $N$ -boson ground states close to the unitary limit [8]. In particular, the binding energy  $E_N$  of the  $N$ -boson ground state increases geometrically with  $N$ :

$$\frac{E_{N+1}}{E_N} \approx 8.567, \quad N \gg 1. \quad (5)$$

Thus, the separation energy for one particle is approximately 88% of the total binding energy. This is in contrast to most other physical systems, where the ratio of the single-particle separation energy to the total binding energy decreases to zero as the number of particles increases. The numbers  $E_3^{(0)}/E_2 = 16.5$  and  $E_4^{(0)}/E_3^{(0)} = 11.9$  obtained from the exact 3-body and 4-body results in Eqs. (3) and (4) appear to be converging toward the universal prediction for large  $N$  in Eq. (5). In Ref. [12],  $E_N$  was explicitly calculated up to  $N = 10$  in lattice effective field theory and found to be consistent with Eq. (5). In any real physical system, however, the relation (5) can only be valid up to some maximum value of  $N$  determined by the range of the underlying interaction. When the states become compact enough that short-distance properties are probed, the binding energy will no longer be universal. In particular, for Lennard-Jones potentials and realistic Helium-Helium potentials, effective range effects can be quite large for three and more particles and the universal limit is approached only slowly [13].

In experiments with cold atoms in a trap, the quasi- $2d$  limit can be reached by special trap geometries. The influence of a trapping potential on ultracold gases in this limit was extensively studied by Petrov and collaborators [14–16]. Although these works are mainly concerned with many-body effects in two-dimensional systems, they have applications for few-body aspects as well.

In this paper, we concentrate on strictly two-dimensional systems of bosons neglecting any trapping effects. We calculate three-body observables close to unitarity in the framework of an effective field theory for large scattering length. We are especially interested in the leading non-universal corrections due to effective range effects. They enter at next-to-leading order in the effective field theory. Such effects must be under control for the experimental

observation of universal phenomena in  $2d$ . In particular, we calculate the leading non-universal corrections to the three-body binding energies, the boson-dimer scattering phase shift and effective range parameters, and the three-body recombination rate for finite energy.

## II. METHOD

In this section, we briefly review the derivation of the three-body equations for  $d = 2$  in effective field theory. (See, e.g., Refs. [8, 17] for more details.) For convenience, we set  $\hbar = 1$  in the following equations. We include a boson field  $\Psi$  and an auxiliary dimer field  $d$  in the Lagrangian. Since we include effective range effects, the dimer field is dynamical:

$$\mathcal{L} = \Psi^\dagger \left( i\partial_t + \frac{\nabla^2}{2m} \right) \Psi + d^\dagger \left( \eta \left( i\partial_t + \frac{\nabla^2}{4m} \right) + \Delta \right) d - \frac{g}{4} (d^\dagger \Psi^2 + \Psi^\dagger 2 d) + \dots, \quad (6)$$

where the dots indicate higher order terms,  $m$  is the mass of the particles,  $\eta = \pm 1$ , and  $\Delta$  and  $g$  denote the bare coupling constants. The sign  $\eta$  can be used to tune the sign of the effective range term. Negative  $\eta$  leads to positive values of the effective range  $r^2$ . In this case, the dimer kinetic term has a negative sign and the dimer field is a ghost. We will come back to this issue below. Note that three-body interactions enter only at higher orders and are not considered in this work.

The  $2d$  effective range expansion, Eq. (1), can also be written in terms of the binding wave number  $\kappa = \sqrt{m E_2}$ :

$$\cot \delta(k) = \frac{2}{\pi} \ln \left( \frac{k}{\kappa} \right) + \frac{r^2}{2\pi} (\kappa^2 + k^2) + \mathcal{O}(k^4). \quad (7)$$

We can deduce the dependence of the binding wave number on the scattering length and the effective range from Eqs. (1) and (7),

$$\kappa = -\frac{i}{r} \sqrt{2 W \left( -2e^{-2\gamma_E} \frac{r^2}{a^2} \right)} \approx \frac{2e^{-\gamma_E}}{a} \sqrt{1 + 2e^{-2\gamma_E} \frac{r^2}{a^2}}, \quad (8)$$

where the signs are chosen such that  $\kappa > 0$ . The function  $W$  is the product logarithm or Lambert  $W$ -function. It is defined as the solution to  $z = we^w$ , namely  $W(z) = w$ . In the limit  $r^2 \rightarrow 0$  the expression for  $E_2$  reduces to Eq. (2) and  $\kappa \approx 1.1229/a$ .

The Lagrangian in Eq. (6) implies the following Feynman rules: The propagator for a boson with energy  $k_0$  and wave number  $\mathbf{k}$  is given by  $i/(k_0 - k^2/(2m) - i\epsilon)$ , where  $k = |\mathbf{k}|$ . The bare dimer propagator is  $i/(\eta(k_0 - k^2/(4m)) + \Delta)$  and the boson-dimer vertex coupling is given by  $-ig/2$ . Because the scattering length is large, boson loops are not suppressed and the bare propagator has to be dressed by boson bubbles to all orders. The full dimer propagator can be obtained by solving the integral equation in Fig. 2. This leads to the expression

$$iD(p_0, p) = -i \frac{32\pi}{mg^2} \left\{ \ln \left[ \frac{p^2/4 - mp_0 - i\epsilon}{\kappa^2} \right] + \frac{r^2}{2} (\kappa^2 + mp_0 - p^2/4) \right\}^{-1}, \quad (9)$$

where we have already matched  $g$  and  $\Delta$  to the effective range expansion, Eq. (7). The wave function renormalization constant is given by the residue of the bound state pole in



FIG. 2: Integral equation for the full dimer propagator (thick solid line). The bare dimer propagator and the boson propagator are indicated by double and single lines, respectively.

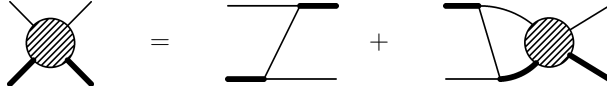


FIG. 3: Integral equation for the boson-dimer scattering amplitude. The boson (full dimer) propagators are indicated by the solid (thick solid) lines. The external lines are amputated.

the propagator (9):

$$Z = \frac{32\pi}{m^2 g^2} \frac{2\kappa^2}{2 - \kappa^2 r^2}. \quad (10)$$

The boson-dimer scattering amplitude is given by the integral equation in Fig. 3, which iterates the one-boson exchange to all orders. Using the Feynman rules from above and projecting onto  $S$ -waves, we obtain [8, 17]:

$$\begin{aligned} T(p, k; E) = & \frac{16\pi}{m} \frac{\kappa^2}{2 - \kappa^2 r^2} \frac{1}{\sqrt{(p^2 + k^2 - mE)^2 - p^2 k^2}} \\ & + 4 \int_0^\infty \frac{dq q T(q, k; E)}{\sqrt{(p^2 + q^2 - mE)^2 - p^2 q^2}} \\ & \times \left( \ln \left[ \frac{\frac{3}{4}q^2 - mE - i\epsilon}{\kappa^2} \right] + \frac{r^2}{2} \left( \kappa^2 + mE - \frac{3}{4}q^2 \right) \right)^{-1}, \end{aligned} \quad (11)$$

where  $k$  ( $p$ ) are the relative wave numbers of the incoming (outgoing) boson and dimer in the center-of-mass system and  $E$  is the total energy. The amplitude  $T(p, k; E)$  has simple poles at negative energies corresponding to three-body bound states. A more general discussion of the analytic properties of few-body scattering amplitudes in  $2d$  is given in Ref. [18].

The three-body binding energies are most easily obtained from solving the homogeneous version of Eq. (11) for negative energies  $E = -E_3$ :

$$\begin{aligned} B(p; E_3) = & 4 \int_0^\infty \frac{dq q B(q; E_3)}{\sqrt{(p^2 + q^2 + mE_3)^2 - p^2 q^2}} \\ & \times \left( \ln \left[ \frac{\frac{3}{4}q^2 + mE_3}{\kappa^2} \right] + \frac{r^2}{2} \left( \kappa^2 - mE_3 - \frac{3}{4}q^2 \right) \right)^{-1}. \end{aligned} \quad (12)$$

In Eqs. (11) and (12) the effective range  $r^2$  is included nonperturbatively in the denominator of the dimer propagator (9). Both equations therefore contain some higher-order effective range effects but still correspond to next-to-leading order in the effective field theory expansion. At the next higher order, where terms proportional to  $(r^2)^2$  enter, there are also contributions from the  $k^4$  term in the effective range expansion (1), (7) which are not included here.<sup>1</sup>

<sup>1</sup> Note that in three dimensions the  $k^4$  term enters one order higher and the corresponding equation would

The integral equations (11) and (12) can be solved in a straightforward way for negative effective range ( $\eta = 1$ ). For positive effective range ( $\eta = -1$ ), an unphysical deep bound state pole appears in the dimer propagator (9). As the effective range is increased, this pole moves to lower energies. Its appearance is related to a violation of the Wigner causality bound which constrains the value of the effective range  $r^2$  for short-ranged, energy-independent interactions. For a detailed discussion of this bound in general dimension  $d$ , see Refs. [19, 20]. This deep pole appears when we circumvent the Wigner bound by introducing a ghost dimer field ( $\eta = -1$ ). It limits the energy range where our approach is applicable. Identifying the position space cutoff in [19] with  $1/\Lambda$ , the Wigner bound translates to

$$r^2 \leq \frac{2}{\Lambda^2} \{ [\ln(\Lambda a) + 1/2]^2 + 1/4 \} , \quad (13)$$

where  $\Lambda$  is an ultraviolet cutoff on the integration wave numbers in Eqs. (11) and (12). In the limit  $\Lambda \rightarrow \infty$ , the constraint becomes  $r^2 \leq 0$ . There are at least two strategies to deal with this problem:

1. Expand the full dimer propagator (9) to linear order in  $r^2$  and treat the range perturbatively. This removes the deep pole and includes all terms to next-to-leading order.
2. Keep an explicit wave number cutoff  $\Lambda$  in equations (11) and (12) such that Eq. (13) is satisfied. The unphysical pole then has no effect on low-energy observables.

Both strategies are applicable for wave numbers  $|k^2 r^2| \ll 1$ . In the following, we make use of Eqs. (11) and (12) and use strategy 2 to calculate three-body observables. A brief description of the perturbative treatment is given in Appendix A.

### III. THREE-BODY OBSERVABLES

In this section, we present our results for the leading non-universal corrections to the three-boson binding energies, the boson-dimer scattering phase shifts and effective range parameters, and the three-boson recombination rate for finite energy. Since we are mainly interested in applications to cold atoms, we will refer to the bosons as atoms in the remainder of the paper.

#### A. Three-body binding energies

We start with the effective range corrections to the three-body binding energies in Eq. (3). For  $r^2 \kappa^2 < 0$ , the energies can straightforwardly be obtained by solving Eq. (12). This is similar to the three-dimensional case investigated in [21]. For  $r^2 \kappa^2 > 0$ , we have to keep track of the Wigner bound. We use an explicit wave number cutoff  $\Lambda$  and vary  $\Lambda$  from  $1/5$  to  $4/5$  of the maximum value determined by the position of the unphysical pole in Eq. (12). This value agrees within a factor of two with the maximum value given by Eq. (13). The

---

be valid to next-to-next-to-leading order. The difference is due to the form of the effective range expansion in two dimensions.

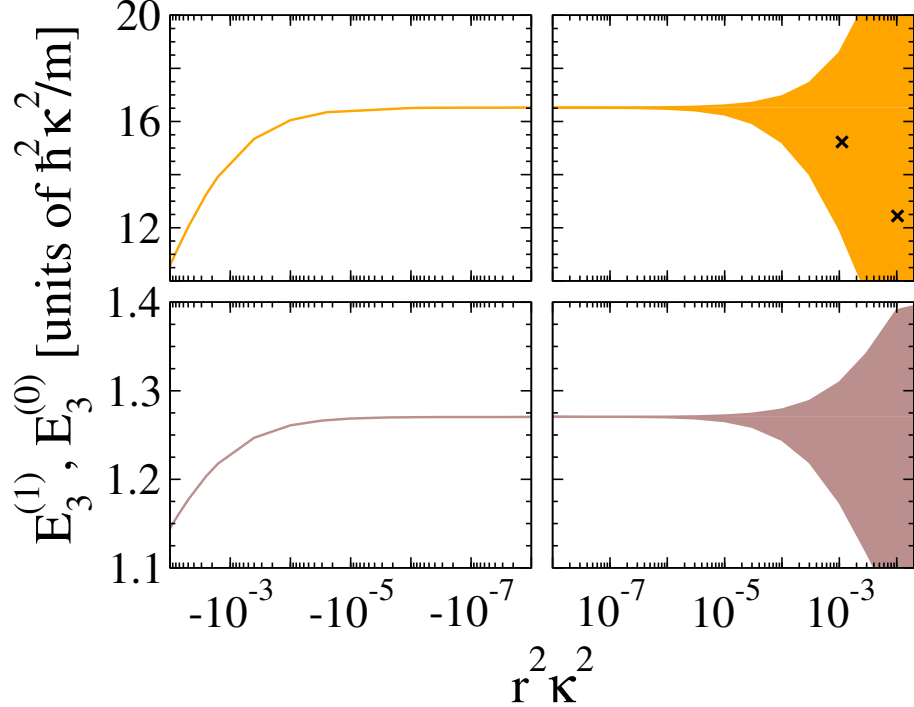


FIG. 4: (Color online) Three-body binding energies  $E_3^{(1)}$  and  $E_3^{(0)}$  in units of  $\hbar^2 \kappa^2 / m$  vs. the two-body effective range  $r^2 \kappa^2$ . The shaded bands are derived with the help of cutoff variation as described in the text and provide an error estimate. The crosses are Monte Carlo results for the modified KORONA potential from [13, 23].

dependence of the three-body energies on the cutoff is monotonic. The smallest cutoff results in the smallest energy value whereas the largest cutoff results in the largest energy. This cutoff variation allows us to check whether the calculation is converged with respect to the cutoff and gives an error estimate for our results. We note that one still has to be careful about possible artefacts from the iteration of range terms. In the  $3d$  case, it was shown that the ultraviolet behavior of the integral-equation kernel is already modified for momenta well below  $1/r$  [22].

Our results for the three-body binding energies  $E_3^{(1)}$  and  $E_3^{(0)}$  as a function of the effective range,  $r^2 \kappa^2$ , are summarized in Fig. 4. For negative effective range  $r^2 \kappa^2$ , both three-body states become less bound as  $|r^2 \kappa^2|$  is increased. This behavior is quantitatively similar to the dimer state, cf. Eq. (8). The binding energies are very sensitive to the effective range. For  $r^2 \kappa^2 = -0.01$ , we find the values  $E_3^{(1)} = 1.145(1) E_2$  for the excited state and  $E_3^{(0)} = 10.578(1) E_2$  for the ground state. For this rather small effective range, the ground state energy has already shifted by about 30% while the excited state energy is shifted by about 10%. This sensitivity is partially related to the special nature of the effective range term in  $2d$  which has units of [length] $^2$ . Taking the square root, the leading range correction of 10 – 30% for  $|r\kappa| = 0.1$  looks more natural. Our calculation including the leading non-universal corrections suggests that the three-body states eventually cross the atom-dimer threshold as the effective range is made more negative. For the excited state this happens around  $r^2 \kappa^2 \approx -0.4$ , but higher order corrections are expected to be important. If this behavior holds true and the effective range could be varied in experiment, the three-body

states in  $2d$  might be observable through zero energy scattering resonances similar to Efimov states in  $3d$ . For positive values of the effective range, the central value of our error band also corresponds to a less strongly bound system but we can not make a definite prediction. Once the effective range effects become appreciable, the errors in our calculation become too large. However, the Monte Carlo results for the modified KORONA potential from [13, 23] (see the crosses in Fig. 4) are in good agreement with our band. They also give a diminishing energy for larger positive effective range. Note that we only show the two points from [13] closest to the unitary limit. All other data points are outside the range of  $r^2\kappa^2$  displayed in Fig. 4.

For effective ranges close to zero, the binding energies depend linearly on  $r^2\kappa^2$ . We can determine the coefficient of the leading term numerically to about 15% accuracy. For  $r^2\kappa^2 < 0$ , we find:

$$\begin{aligned} E_3^{(0)}/E_2 &= 16.522688(1) + 28000(5000) r^2\kappa^2 + \mathcal{O}(r^4\kappa^4), \\ E_3^{(1)}/E_2 &= 1.2704091(1) + 540(80) r^2\kappa^2 + \mathcal{O}(r^4\kappa^4). \end{aligned} \quad (14)$$

For  $r^2\kappa^2 > 0$ , the coefficient of  $r^2\kappa^2$  can not be extracted from our calculation. While the values of  $E_3^{(0)}$  and  $E_3^{(1)}$  are very insensitive to the cutoff variation at small positive  $r^2\kappa^2$ , even the sign of the slope is not well determined. We note that  $r^2\kappa^2$  can be quite small in  $2d$  systems even if the effective range is substantially larger than the range of the interaction (see, e.g., the explicit example of a circular well potential given in Sec. 6.1 of Ref. [20]). The large coefficients in Eq. (14), however, cause significant effective range corrections already for  $|r^2\kappa^2|$  of order  $10^{-4}$  to  $10^{-3}$ .

## B. Atom-dimer scattering

Next, we consider the effective range corrections to elastic atom-dimer scattering. We find scattering observables in general to be less sensitive to the unphysical deep poles. To obtain the scattering amplitude, we solve Eq. (11) for  $E = \frac{3}{4m}k^2 - E_2$  below the dimer breakup threshold with the incoming particles on-shell. The elastic scattering phase shift  $\delta_{AD}(k)$  can then be obtained from the scattering amplitude for  $p = k$  using

$$T\left(k, k; \frac{3}{4m}k^2 - E_2\right) = \frac{3}{m}f_k = \frac{3}{m} \frac{1}{\cot \delta_{AD}(k) - i}. \quad (15)$$

In Fig. 5, we show  $\cot \delta_{AD}$  for different values of  $r^2\kappa^2$  as a function of the wave number  $k$  up to the dimer breakup threshold  $k \approx 1.15\kappa$ . For small values of  $k$ ,  $\cot \delta_{AD}$  is almost linear in  $\ln k$  but at about half the breakup wave number the behavior becomes more complicated. For  $r^2\kappa^2 < 0$ , the non-universal corrections increase  $\cot \delta_{AD}$  compared to the universal result while for  $r^2\kappa^2 > 0$  the behaviour depends on the value of  $r^2\kappa^2$ .

The atom-dimer effective range parameters can be extracted from our results by fitting the effective range expansion, Eq. (1), to  $\cot \delta_{AD}$ . We have performed fits with different orders in the expansion and different truncations of the data sets to estimate the error in this extraction. Our results for  $\kappa a_{AD}$  and  $(\kappa r_{AD})^2$  in dependence of  $r^2\kappa^2$  are summarized in Fig. 6. The effective range  $r_{AD}^2$  comes out positive for all values of  $r^2\kappa^2$  considered. For  $|r^2\kappa^2| \lesssim 10^{-4}$  the curves are nearly symmetric around  $r^2\kappa^2 = 0$  and can be approximated by

$$\kappa a_{AD} = 2.614(1) - 4100(500) r^2\kappa^2 + \mathcal{O}(r^4\kappa^4). \quad (16)$$

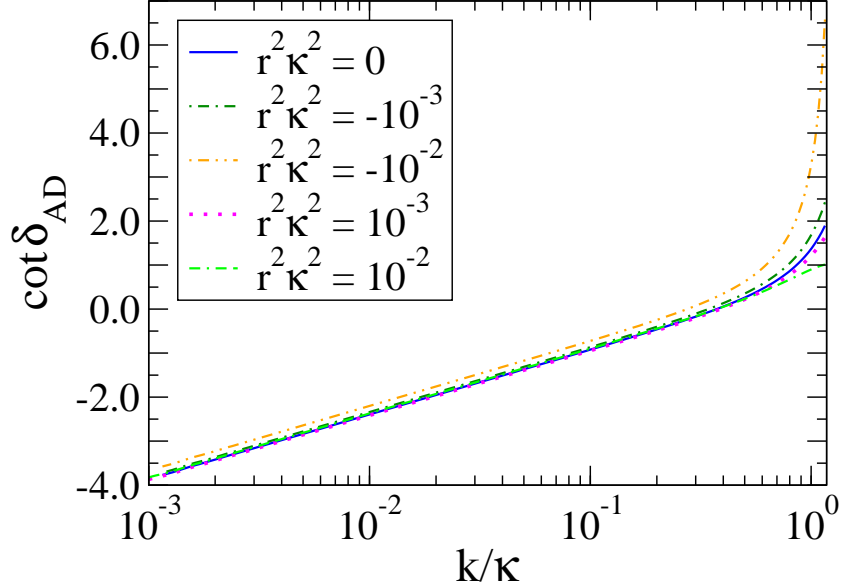


FIG. 5: (Color online) The elastic atom-dimer scattering phase shift  $\cot \delta_{AD}$  for  $r^2 \kappa^2 = 0, \pm 10^{-3}, \pm 10^{-2}$  as a function of the wave number  $k/\kappa$ .

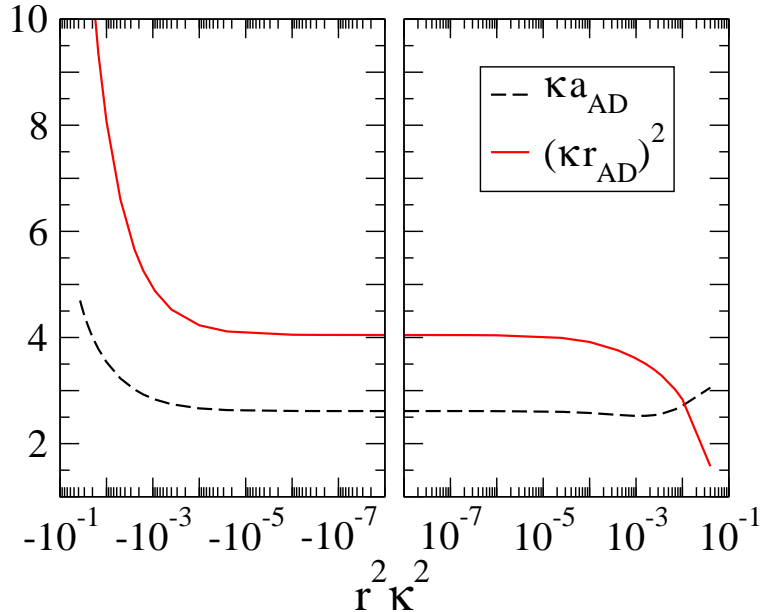


FIG. 6: (Color online) The atom-dimer scattering length  $\kappa a_{AD}$  and effective range  $(\kappa r_{AD})^2$  as a function of the two-body effective range  $r^2 \kappa^2$ .

Similar to the bound state case, we find large coefficients in the perturbative expansion in  $r^2 \kappa^2$ . For larger values of  $r^2 \kappa^2$ , the curves are not symmetric anymore. In the unitary limit, we find the effective range parameters  $\kappa a_{AD} = 2.614(1)$  and  $(\kappa r_{AD})^2 = 4.0(2)$ . Converting to units of the scattering length  $a$ , our results correspond to  $a_{AD} = 2.328(1) a$  and  $\ln(a_{AD}/a) = 0.845(1)$ . These numbers agree well with the value  $\ln(a_{AD}/a) = 0.8451$  obtained by Kartavtsev et al. [11] and are in qualitative agreement with the value  $a_{AD} = 2.95a$  found by Nielsen et al. [6]. For  $r^2 \kappa^2$  of order 0.01, there are again substantial effective

range effects. In particular, we find the values  $\kappa a_{AD} = 3.540(1)$  and  $(\kappa r_{AD})^2 = 7.4(2)$  for  $r^2\kappa^2 = -0.01$  and  $\kappa a_{AD} = 2.713(1)$  and  $(\kappa r_{AD})^2 = 2.9(2)$  for  $r^2\kappa^2 = 0.01$ .

We have also calculated the atom-dimer scattering phase shifts and effective range parameters using the fully perturbative treatment discussed in Appendix A. For sufficiently small effective range, the two methods agree.

### C. Three-body recombination

Finally, we consider three-body recombination into the shallow dimer described by Eq. (2). Cold atoms typically also have a large number of deep dimer states. However, three-body recombination into the deep dimers is suppressed since the atoms have to approach to distances comparable to the size of the deep dimers. This process enters at the same order as short-range three-body interactions. It could be calculated by introducing a complex three-body parameter [17].

The three-body recombination into the shallow dimer is strongly influenced by the behavior of the full dimer propagator, Eq. (9). There are three limits in which the propagator vanishes: (i)  $a \rightarrow \infty$ , (ii)  $E \rightarrow 0$ , and (iii)  $E \rightarrow \infty$ . In these three limits, the three-body recombination rate also vanishes. For large but finite scattering length and finite energy, however, three-body recombination can take place.

The rate can be conveniently calculated using the inelastic atom-dimer scattering cross section [24]. The integration measure of the three-body phase space in two dimensions using hyperspherical variables is given by

$$d^2p_1 d^2p_2 d^2p_3 = m^2 E \sin(2\alpha_3) dE d\alpha_3 d\varphi_{12} d\varphi_{3,12} d^2p_{tot}. \quad (17)$$

From this, the relation between the hyperangular average of the recombination rate at finite energy and the inelastic cross section in two dimensions is obtained as

$$K(E) = \frac{36\pi}{m^2 E} k \sigma_{AD}^{(\text{inel})}(E), \quad (18)$$

where  $k = \sqrt{\frac{4m}{3}(E + E_2)}$ . The inelastic cross section in Eq. (18) can be obtained by subtracting the elastic cross section

$$\sigma_{AD}^{(\text{el})}(E) = \frac{4}{k} |f_k|^2, \quad (19)$$

from the total cross section  $\sigma_{AD}^{(\text{tot})}(E)$ . The latter can be obtained from the optical theorem which in 2d is given by [25]

$$\sigma_{AD}^{(\text{tot})}(E) = \frac{4}{k} \text{Im} f_k(0). \quad (20)$$

Using the expression for the elastic scattering amplitude, Eq. (15), the three-body recombination rate  $K(E)$  can be calculated from Eqs. (18), (19), and (20). Our results for  $K(E)$  as a function of the wave number  $k$  are shown in Fig. 7. For positive  $r^2\kappa^2$ , we again make use of a cutoff variation in the range of 1/5 to 4/5 of the maximum allowed value. The grey band gives our result for  $r^2\kappa^2 = 10^{-4}$ . For larger values of  $r^2\kappa^2$ , the width of the band increases. As expected, the rate vanishes for large wave numbers and at threshold. Around  $k \approx 3\kappa - 4\kappa$ , there is a maximum in the recombination rate. The position of the maximum

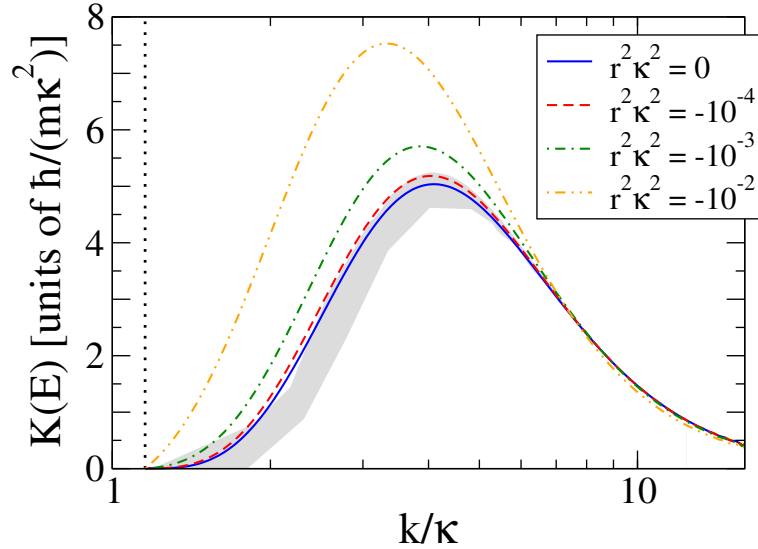


FIG. 7: (Color online) The energy-dependent three-body recombination rate  $K(E)$  in units of  $\hbar/(m\kappa^2)$  as a function of the wave number  $k/\kappa$ . The shaded band corresponds to  $r^2\kappa^2 = 10^{-4}$  and is derived with the help of cutoff variation as described in the text.

is weakly dependent on the value of the effective range. It is governed by the behavior of the full dimer propagator as a function of the energy, Eq. (9). The maximum is not related in a simple way to the energy of the universal three-body states, Eq. (3), but our calculation establishes an implicit relation between the two.

In experiments with cold atoms, one typically uses ensembles of atoms in thermal equilibrium. The energy-dependent recombination rate  $K(E)$  can be converted into an energy averaged rate by performing a Boltzmann average as described in Ref. [24]. Taking into account the energy dependence of the three-body phase space, Eq. (17), we have

$$\begin{aligned} \alpha(T) &= \frac{\int_0^\infty dEEe^{-E/(k_B T)} K(E)}{3! \int_0^\infty dEEe^{-E/(k_B T)}} \\ &= \frac{1}{6k_B^2 T^2} \int_0^\infty dEEe^{-E/(k_B T)} K(E). \end{aligned} \quad (21)$$

Our results for  $\alpha(T)$  for different values of the effective range are shown in Fig. 8. We do not give results for  $r^2\kappa^2 > 0$  but the shaded band for  $r^2\kappa^2 = 10^{-4}$  in Fig. 7 translates into an error band around  $r^2\kappa^2 = 0$  here as well. The temperature dependent rate also has a maximum at temperatures of the order of 5...7 times the dimer binding energy. The recombination rate at the maximum is very sensitive to the value of the effective range. If the effective range is changed from zero to  $r^2\kappa^2 = -0.01$ , the rate at the maximum changes by a factor of two. For all values of the effective range considered, however, the recombination rate at the maximum remains of order one in natural units  $\hbar/(m\kappa^2)$ . This suggests that 2d Bose gases are stable enough to observe universal few-body phenomena experimentally. The lifetime of a 2d Bose gas with large scattering length was previously estimated by Pricoupenko and Olshanii [26]. The order of magnitude of our recombination rates is consistent with their results.

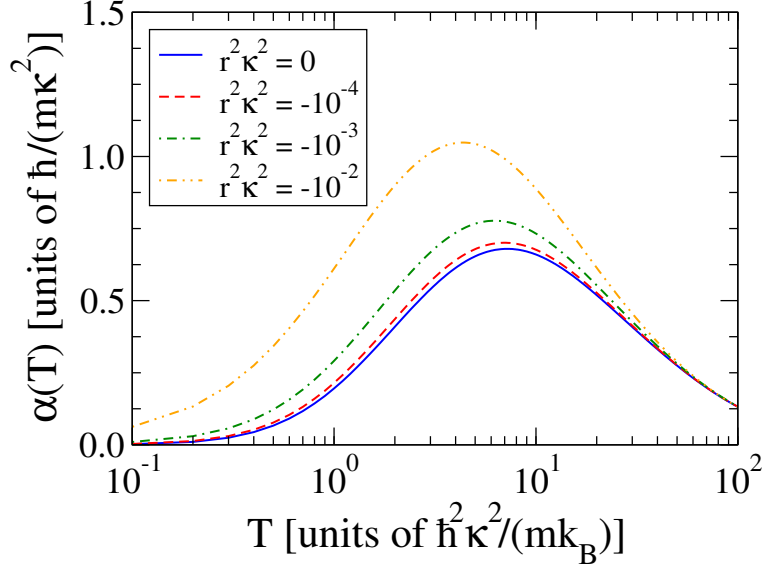


FIG. 8: (Color online) The three-body recombination rate  $\alpha$  in units of  $\hbar/(mk^2)$  in dependence of the temperature  $T$  in units of  $\hbar^2\kappa^2/(mk_B)$ .

#### IV. SUMMARY & CONCLUSIONS

In this work, we have investigated the three-body properties of identical bosons close to the unitary limit in two spatial dimensions. Within an effective field theory for resonant interactions, we have calculated the leading non-universal corrections which are due to the two-body effective range. In particular, we have calculated the leading corrections to the three-body binding energies, the atom-dimer scattering phase shift and effective range parameters, and the three-body recombination rate at finite energy.

We have compared our results to previous calculations in the unitary limit where available and generally found good agreement. Our calculations show a large sensitivity of three-body observables to the effective range. Significant effective range effects can be observed already for  $|r^2\kappa^2| \gtrsim 10^{-4} - 10^{-3}$ . These corrections are due to large coefficients in the perturbative expansion of observables in  $r^2\kappa^2$  (cf. Eqs. (14), (16)). It would be interesting to understand the physics behind these large coefficients. These coefficients could be reduced by an order of magnitude by renormalizing to the three-body ground state energy  $E_3^{(0)}$  instead of  $E_2$  [27], but they would still remain unnaturally large. Our results suggest that the approach to the unitary limit in  $2d$  three-body observables is rather slow and effective range corrections play an important role even close to the unitary limit. This is in agreement with the results of Blume who investigated the universal properties of  $N$ -body droplets using Lennard-Jones potentials and realistic Helium potentials [13].

Our calculation of the three-body energies including the leading non-universal corrections suggests that the bound states eventually cross the atom-dimer threshold as the effective range is made more negative. If this behavior holds true when higher orders are included, it opens the possibility to observe three-body states in  $2d$  through a variation of the  $2d$  effective range. The states would then appear as zero energy scattering resonances similar to Efimov states in  $3d$ .

Our results are directly applicable to two-dimensional Bose gases with large scattering

length and imply that effective range effects must be under control in experiments on universal properties of  $2d$  Bose gases. Effective field theory provides a powerful tool to calculate these corrections and our study provides the first step towards accurate calculations of these effects.

On the experimental side, there has been some progress in the study of universal properties of  $2d$  Bose gases. For example, Chin and coworkers have recently studied scale invariance and critical behavior near a Berezinsky-Kosterlitz-Thouless phase transition in  $2d$  and observed universal behavior of the thermodynamic functions [28]. They have also attempted to show how the Efimov resonance in three-body recombination shifts when the system is tuned towards a dimensionality of two by increasing one of the trapping frequencies in a  $3d$  experiment [29].

Interesting few-body properties of  $2d$  systems include universal  $N$ -body states and a geometric spectrum of  $N$ -body ground states [8]. Moreover, Nishida and Tan have shown that a two-species Fermi gas in which one species is confined in  $2d$  or  $1d$  while the other is free in the three-dimensional space is stable against the Efimov effect and has universal properties [30]. More complicated multispecies Fermi gases with similar properties are possible as well. They also showed that a purely  $S$ -wave resonance in  $3d$  can induce higher partial wave resonances in mixed dimensions and pointed out that some of the resonances observed in a recent experiment by the Florence group [31] can be interpreted as a  $P$ -wave resonance in mixed  $2d$ - $3d$  dimensions [32]. Thus, future experiments considering few-body phenomena in lower-dimensional ultracold gases will be very interesting. Our calculation of the leading non-universal corrections provides a basis for the interpretation of such experiments.

### Acknowledgments

We thank Y. Nishida, L. Pricoupenko, and D. Phillips for discussions and D. Blume for providing her data. We are also grateful to the INT in Seattle for hospitality during the program “Simulations and Symmetries: Cold Atoms, QCD, and Few-hadron Systems” where part of this work was done. K.H. was supported by the “Studienstiftung des deutschen Volkes” and by the Bonn-Cologne Graduate School of Physics and Astronomy.

### Appendix A: Perturbative treatment

It is also possible to include the effective range in a fully perturbative way. In order to achieve this, we expand the boson-dimer scattering amplitude into a leading order piece  $T_0(p, k; E)$  which satisfies Eq. (11) with  $r^2 \equiv 0$  and a correction  $T_2(p, k; E)$  of order  $r^2$ :

$$T(p, k; E) = T_0(p, k; E) + T_2(p, k; E) + \dots . \quad (\text{A1})$$

Next, we insert this expansion (A1) into Eq. (11), expand the  $r^2$  dependent terms, and collect all terms of order  $r^2$  in order to obtain an equation for  $T_2(p, k; E)$ . The on-shell scattering amplitude at next-to-leading order can then be written as an integral over the

leading order amplitude and we finally obtain:

$$T(k, k; E) = \left(1 + \frac{r^2 \kappa^2}{2}\right) T_0(k, k; E) - \frac{mr^2}{4\pi\kappa^2} \int_0^\infty dq q \left(\kappa^2 + mE - \frac{3}{4}q^2\right) \left[ \frac{T_0(k, q; E)}{\ln\left((\frac{3}{4}q^2 - mE - i\epsilon)/\kappa^2\right)} \right]^2, \quad (\text{A2})$$

where  $E = 3k^2/(4m) - E_2$ . The scattering phase shift can be extracted using Eq. (15) as before.

---

[1] I. Bloch, J. Dalibard, and W. Zwerger, Rev. Mod. Phys. **80**, 885 (2008) [arXiv:0704.3011v2 [cond-mat.other]].

[2] F. Ferlaino and R. Grimm, Physics **3**, 9 (2010).

[3] T. Esslinger, Ann. Rev. Cond. Mat. Phys. **1**, 129 (2010) [arXiv:1007.0012 [cond-mat.quant-gas]] and references therein.

[4] V. Efimov, Phys. Lett. **33B**, 563 (1970).

[5] L.W. Bruch and J.A. Tjon, Phys. Rev. A **19**, 425 (1979).

[6] E. Nielsen, D.V. Fedorov, and A.S. Jensen, Few-Body Syst. **27**, 15 (1999).

[7] B.J. Verhaar, L.P.H. de Goey, E.J.D. Vredenbregt, and J.P.H.W. van den Eijnde, J. Phys. A: Math. Gen. **17**, 595 (1984).

[8] H.-W. Hammer and D.T. Son, Phys. Rev. Lett. **93**, 250408 (2004) [arXiv:cond-mat/0405206].

[9] L. Platter, H.-W. Hammer, Ulf-G. Meißner, Few-Body Syst. **35**, 169 (2004) [arXiv:cond-mat/0405660v2].

[10] I.V. Brodsky, M.Yu. Kagan, A.V. Klaptsov, R. Combescot, and X. Leyronas, Phys. Rev. A **73**, 032724 (2006).

[11] O.I. Kartavtsev and A.V. Malykh, Phys. Rev. A **74**, 042506 (2006) [arXiv:physics/0606013].

[12] D. Lee, Phys. Rev. A **73**, 063204 (2006) [arXiv:physics/0512085].

[13] D. Blume, Phys. Rev. B **72**, 094510 (2005) [arXiv:cond-mat/0507729].

[14] D.S. Petrov and G.V. Shlyapnikov, Phys. Rev. A **64**, 012706 (2001) [arXiv:cond-mat/0012091].

[15] D.S. Petrov, M. Holzmann, and G.V. Shlyapnikov, Phys. Rev. Lett. **84**, 2551 (2000) [arXiv:cond-mat/9909344].

[16] D.S. Petrov, M.A. Baranov, and G.V. Shlyapnikov, Phys. Rev. A **67**, 031601(R) (2003) [arXiv:cond-mat/0212061].

[17] E. Braaten and H.-W. Hammer, Phys. Rept. **428**, 259 (2006) [arXiv:cond-mat/0410417].

[18] S.K. Adhikari and W.G. Gibson, Phys. Rev. A **46**, 3967 (1992).

[19] H.-W. Hammer and D. Lee, Phys. Lett. B **681**, 500 (2009) [arXiv:0907.1763 [nucl-th]].

[20] H.-W. Hammer and D. Lee, Annals Phys. **325**, 2212 (2010) [arXiv:1002.4603 [nucl-th]].

[21] D.S. Petrov, Phys. Rev. Lett. **93**, 143201 (2004) [arXiv:cond-mat/0404036].

[22] L. Platter and D.R. Phillips, Few-Body Syst. **40**, 35 (2006) [arXiv:cond-mat/0604255].

[23] D. Blume, private communication (2011).

[24] E. Braaten, H.-W. Hammer, D. Kang, and L. Platter, Phys. Rev. A **78**, 043605 (2008) [arXiv:0801.1732 [cond-mat.other]].

[25] S.K. Adhikari, Am. J. Phys. **54**, 362 (1986).

- [26] L. Pricoupenko and M. Olshanii, *J. Phys. B: At. Mol. Opt. Phys.* **40**, 2065 (2007) [arXiv:cond-mat/0205210].
- [27] M. Birse, private communication.
- [28] C.-L. Hung, X. Zhang, N. Gemelke, and C. Chin, *Nature* **470**, 236 (2011) [arXiv:1009.0016 [cond-mat.quant-gas]].
- [29] C. Chin, talk presented at the ITAMP workshop “Efimov States in Molecules and Nuclei: Theoretical Methods and New Experiments”, Rome, 19-21 Oct. 2009, available at <http://www.cfa.harvard.edu/itamp/efimovschedule.html>
- [30] Y. Nishida, S. Tan, *Phys. Rev. Lett.* **101**, 170401 (2008) [arXiv:0806.2668 [cond-mat.other]].
- [31] G. Lamporesi, J. Catani, G. Barontini, Y. Nishida, M. Inguscio, and F. Minardi, *Phys. Rev. Lett.* **104**, 153202 (2010) [arXiv:1002.0114 [cond-mat.quant-gas]].
- [32] Y. Nishida, S. Tan, *Phys. Rev. A* **82**, 062713 (2010) [arXiv:1011.0033 [cond-mat.quant-gas]].